



## Thermal modeling of the UHP Maksyutov Complex in the south Urals

Mary L. Leech<sup>a,\*</sup>, Ernst Willingshofer<sup>b,1</sup>

<sup>a</sup>*Geological and Environmental Sciences, Stanford University, Stanford, CA 94305-2115, United States*

<sup>b</sup>*Faculty of Earth and Life Sciences, Vrije Universiteit, De Boelelaan 1085, 1081 HV Amsterdam, Netherlands*

Received 15 March 2004; received in revised form 28 June 2004; accepted 6 July 2004

Editor: S. King

### Abstract

Two-dimensional thermal modeling of the subduction and exhumation of the ultrahigh-pressure (UHP) Maksyutov Complex in the south Ural Mountains tests factors influencing the low modern heat flow in the Urals and the feeble preservation of UHP index minerals. Best-fit models are obtained with initial surface heat flow of  $60 \text{ mW m}^{-2}$  indicating that low modern heat flow in the Urals is a recent anomaly. Ultrahigh-pressure metamorphism was modeled at 388 Ma based on new U–Pb SHRIMP dating of zircon; the average modeled exhumation rate for the UHP eclogites to the mid-crust is  $\sim 5.0 \text{ mm/year}$ , much slower than other UHP complexes. The model predicts that cooling during exhumation is strongly dependent on concomitant subduction/underthrusting in the footwall of the UHP unit and normal faulting in the hanging wall. Low radiogenic heat production in the crust and a relatively thin UHP slab (3–10 km) also favor cooling. For Maksyutov, the modeling shows that cooling was controlled by low radiogenic heat production and underthrusting during decompression to lower crustal levels; these cooling mechanisms accompany exhumation despite low exhumation rates ( $\sim 5 \text{ mm/year}$ ) thereby denying the call for fast exhumation in order to preserve UHP index minerals.

© 2004 Elsevier B.V. All rights reserved.

*Keywords:* thermal modeling; ultrahigh-pressure metamorphism; Ural Mountains; U–Pb SHRIMP dating of zircon

### 1. Introduction and motivation for modeling

The Maksyutov Complex is an ultrahigh-pressure (UHP) subduction zone complex in the south Ural

Mountains. Ultrahigh-pressure index minerals such as coesite and diamond have been difficult to identify in Maksyutov and the poor preservation of coesite, diamond, and their pseudomorphs calls into questions which factors during exhumation of UHP complexes are most important in preserving evidence of UHP metamorphism. Fast exhumation and the need for a relatively cool UHP body are generally considered the most important factors for preservation of UHP index

\* Corresponding author. Tel.: +1 650 736 1821; fax: 1 650 725 0979.

*E-mail addresses:* [mary@geo.stanford.edu](mailto:mary@geo.stanford.edu) (M.L. Leech), [ernst.willingshofer@falw.vu.nl](mailto:ernst.willingshofer@falw.vu.nl) (E. Willingshofer).

<sup>1</sup> Tel.: +31 20 44 47353; fax: +31 20 4449943.

minerals [1]. Based on abundant existing petrologic, geologic, and radiometric data (see following sections), thermal modeling is used to constrain parameters influencing the temperature conditions during UHP body exhumation and to test variables such as exhumation rate, heat production within the crust, and UHP slab thickness.

The general tectonic evolution of the Ural Mountains does not differ from other collisional orogens all over the globe. However, anomalously low modern heat flow (24 to 43 mW m<sup>-2</sup>) along the central axis of the Urals [2] questions the compatibility of present-day heat flow data with the thermal evolution of Maksyutov Complex rocks. Coupled with new radiometric time constraints, we also test with simple

numerical thermal models whether such low heat flow values could permit the observed metamorphism within geologically reasonable conditions. The thermal conditions of subduction and exhumation are critical to understanding all UHP complexes.

## 2. Tectonic framework of Paleozoic collision in the Urals

The Ural Mountains formed as a result of the collision between the East European platform (EEP), microcontinental blocks to the east, and the intervening Magnitogorsk island arc in the Late Devonian to Permian. The Maksyutov Complex is a UHP sub-

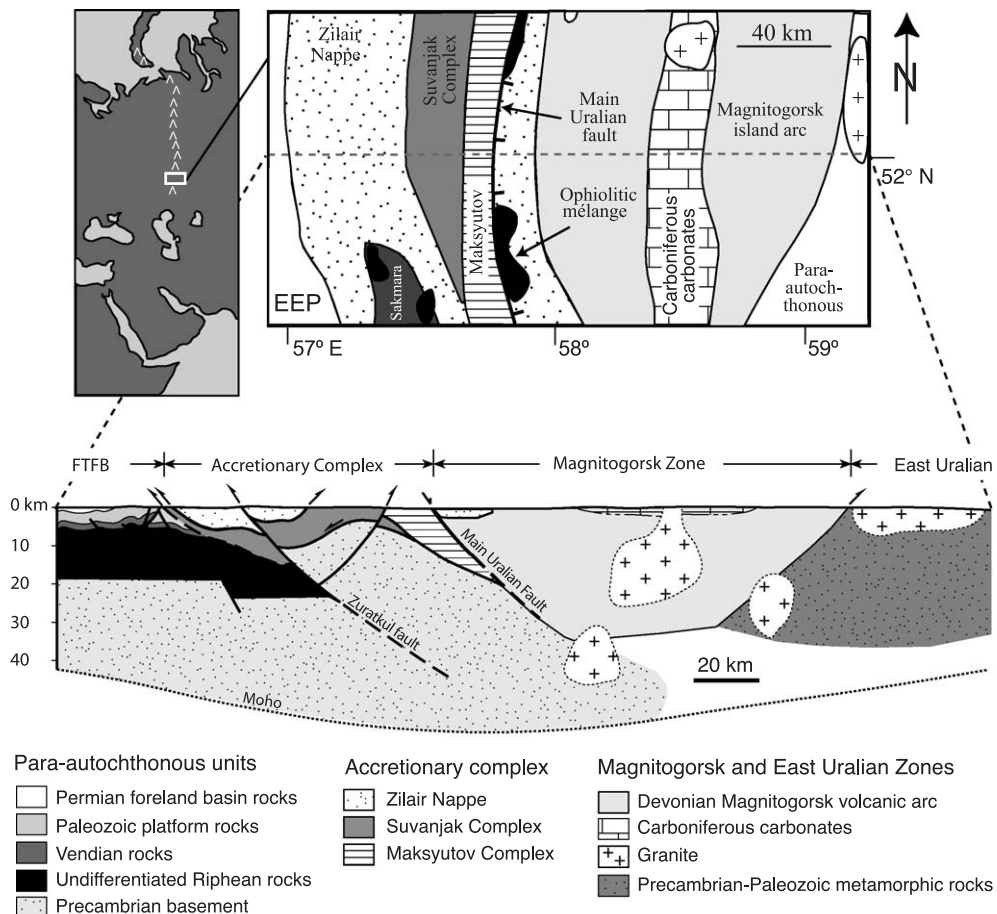


Fig. 1. Cross-section through the south Urals (based on [4]) and a simplified geologic strip map showing the line across the Maksyutov Complex in the south Urals on which modeling was based. Abbreviations: EEP, East European platform; FTFB, foreland fold-and-thrust belt.

duction zone complex that formed upon closure of the Uralian Ocean [3]. The Main Uralian fault (MUF) suture zone extends over 2000 km along the central axis of the 400–450-km-wide orogen; in the south Urals, the MUF juxtaposes the Maksyutov Complex (footwall) with the Magnitogorsk island arc (hanging wall) and associated sedimentary rocks (Fig. 1).

Prior to the Devonian arc-continent collision, the UHP eclogite unit was part of the East European passive margin adjacent to the Uralian Ocean. Rifting and the subsequent opening of the Uralian Ocean occurred from the Cambrian to Early Silurian [5–7] based on the age of alkaline basalts, typical graben facies sediments preserved along the eastern margin of the EEP, and the occurrence of deep-water turbidite

sequences which indicate a rapidly deepening depression within the continental crust in the Sakmara zone west of the Maksyutov Complex [5].

Timing of the initial rifting is recorded in multiple samples from both the eclogitic and serpentinite mélangé unit of the Maksyutov Complex which yield U–Pb zircon SHRIMP ages between about 510 and 550 Ma (see Fig. 2) [8]. The ages likely record rift-related magmatism in the East European platform that resulted in the opening of the Uralian Ocean. The timing of this event corroborates other reports of rifting in the East European platform in the early Cambrian and corresponds well with the age of magmatism associated with ophiolites in the region (e.g., [5]).

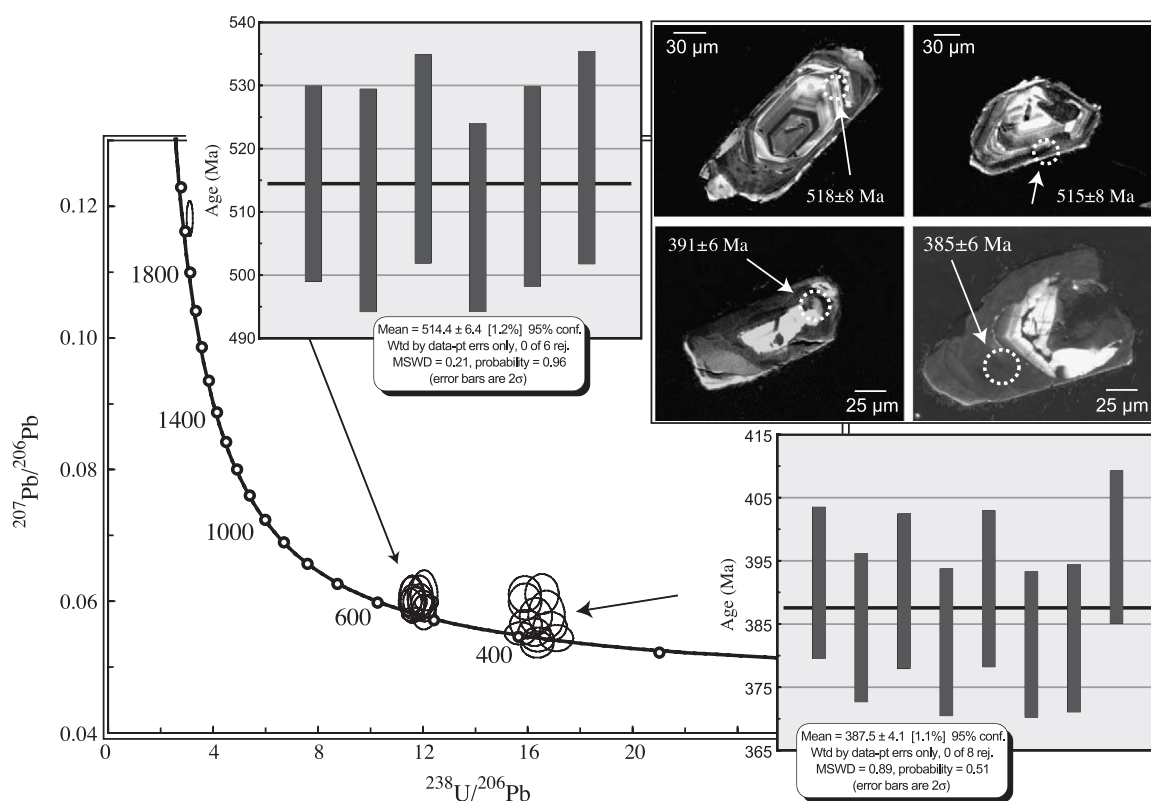


Fig. 2. Tera-Wasserburg concordia diagram showing U–Pb SHRIMP data for 20 zircons from sample UM7a from the UHP eclogite unit of the Maksyutov Complex (error ellipses are  $2\sigma$ ); data are uncorrected for common Pb and analyses high in common Pb were excluded. Weighted mean ages of  $388 \pm 4$  and  $514 \pm 6$  Ma represent  $^{207}\text{Pb}$  corrected ages of individual spots on eight and six zircons, respectively. Ages around 388 Ma are interpreted as the age of UHP metamorphism; ca. 514 Ma ages likely represent rift-related magmatism. Cathodoluminescence images of representative zircons show analyzed points that yielded ca. 388 and 514 Ma ages.

Thrust stacking and the emplacement of oceanic lithosphere was occurring between the Late Silurian and the earliest Devonian; this timing is supported by the presence of ophiolitic debris in the Upper Silurian and Middle Devonian sequences of the Sakmara zone [5]; the Uralian Ocean had closed completely by the Early Devonian (ca. 400 Ma) based on dating of crustal melts generated by ophiolite emplacement along the suture zone [9].

After subduction of the Uralian Ocean, the former European passive margin containing the Maksyutov Complex, was subducted to depths suitable for UHP metamorphism. Collision may have continued until the Late Devonian based on clastics in the Zilair Formation [10]; early-stage exhumation of the UHP rocks from HP eclogite- to blueschist-/greenschist-facies conditions in the late Early–Late Devonian rocks may therefore have been syn-convergent, corresponding to evidence from fission-track dating [11]. Minor normal movement on the MUF probably helped exhume the Maksyutov Complex, but activity on the fault likely ended by ~300 Ma [11,12]. The structural association of tectonic units (Fig. 1) as we find them today was established during exhumation of the UHP rocks (see Fig. 5 in [3]).

### 3. Petrologic and radiometric constraints for modeling the Maksyutov UHP unit

The timing for major events in the evolution of the Maksyutov Complex used in the numerical modeling is summarized in Table 1 and Fig. 3. Relevant petrologic and radiometric data are presented below; the data for peak metamorphism and exhumation

define the boxes in Fig. 4 that the models must pass through to be valid.

#### 3.1. Rifting and opening of the Uralian Ocean (Table 1)

Timing of the rifting in the East European platform that resulted in the opening of the Uralian Ocean is recorded in relict igneous zircons from the UHP unit of the Maksyutov Complex. U–Pb SHRIMP dating of these zircons yields ages between  $514 \pm 6$  and  $532 \pm 7$  Ma (see Fig. 2) [8] which we use in the model to constrain the rifting and opening of the Uralian Ocean (Table 1).

#### 3.2. Timing of UHP metamorphism (Figs. 2, 3b and 4; Table 1) and new SHRIMP-RG dating for Maksyutov

The eclogite unit of the Maksyutov Complex experienced UHP metamorphism based on reports of coesite pseudomorphs [14,15], graphite pseudomorphs after diamond [16], and most recently microdiamond aggregate inclusions in garnet [17] indicating minimum pressures of 3.0 GPa. This UHP metamorphic event took place at  $388 \pm 4$  Ma based on new U–Pb SHRIMP dating of zircon (Fig. 2, Table 1; see [8]); these new data date peak metamorphism about 8 to 13 Ma earlier than others have reported (see below) [18,19].

Zircons used for U–Pb dating of the UHP eclogite unit are from three samples of quartzofeldspathic gneiss and mica schist. Zircons are rounded, slightly irregular-shaped grains that display dark rims under cathodoluminescence; some grains show zoned, sometimes euhedral, cores within thin rims (Fig. 2).

Table 1  
Model kinematics and displacement rates for UHP metamorphism

Time (Ma)	Tectonic events	Kinematics	Displacement rate (mm/year)
<i>Model A—UHP metamorphism</i>			
540–514	Opening of Uralian Ocean	200 km pure shear extension	8.00
514–437	Thermal relaxation	N.A.	N.A.
437–398	Subduction of Uralian Ocean	572 km simple shear compression	15.00
398–388	Thermal relaxation/UHP metamorphism	N.A.	N.A.
388–380	Exhumation of UHP rocks to HP conditions	Exhumation by thrusting (buoyant rise)	5.00
380–375	Exhumation of HP rocks to lower/mid-crustal level	Exhumation by thrusting (buoyant rise)	4.50
375–315	Cooling and continued exhumation of UHP rocks	Exhumation by thrusting and erosion	0.47

Early Devonian ages with a weighted mean of  $388 \pm 4$  Ma are derived from dark, rounded grains and dark rims with very low Th/U ratios ( $\ll 0.1$ ) indicating a metamorphic origin (Fig. 2). Weighted

mean ages between  $514 \pm 6$  and  $532 \pm 7$  Ma from UHP unit zircons have much higher Th/U ratios ( $\sim 0.5$ – $1.5$ ) and distinctive oscillatory zoning indicating an inherited igneous component (Fig. 2) [8].

### 3.3. Thermobarometry and the HP eclogite-facies metamorphic event (Fig. 4, Table 1)

Standard thermobarometry on Maksyutov eclogites yields equilibrium temperatures ranging from  $594$  to  $637$  °C and minimum pressure estimates of  $1.5$  to  $1.7$  GPa [16]. The relatively low temperatures and pressures indicated for Maksyutov eclogites by standard thermobarometry likely record a retrograde metamorphic event after UHP metamorphism.

Garnet-whole rock Sm–Nd dating records an HP eclogite-facies metamorphic event at about  $600$  °C ranging from  $366 \pm 7$  to  $382 \pm 10$  Ma [18,19]. Initial Rb–Sr mineral isochron data [20] corroborated a ca.  $370$ – $380$  Ma age for eclogitization, but more recent work with the Rb–Sr system [21] indicates it records a fluid–rock interaction rather than a traditional closure temperature. The ca.  $380$  Ma event likely records cooling during exhumation and/or a fluid-induced metamorphism at post-peak temperatures ( $\sim 600$  °C); we combine this data with the thermobarometric estimates to constrain the HP eclogite-facies metamorphic event.

### 3.4. Cooling during exhumation and final ascent to the upper crust (Figs. 3c–d and 4; Table 1)

Previous  $^{40}\text{Ar}/^{39}\text{Ar}$  and conventional U–Pb rutile data from other workers yield ages from  $375 \pm 3$  to  $380 \pm 4$  Ma and  $384 \pm 3$  Ma, respectively [19,22],

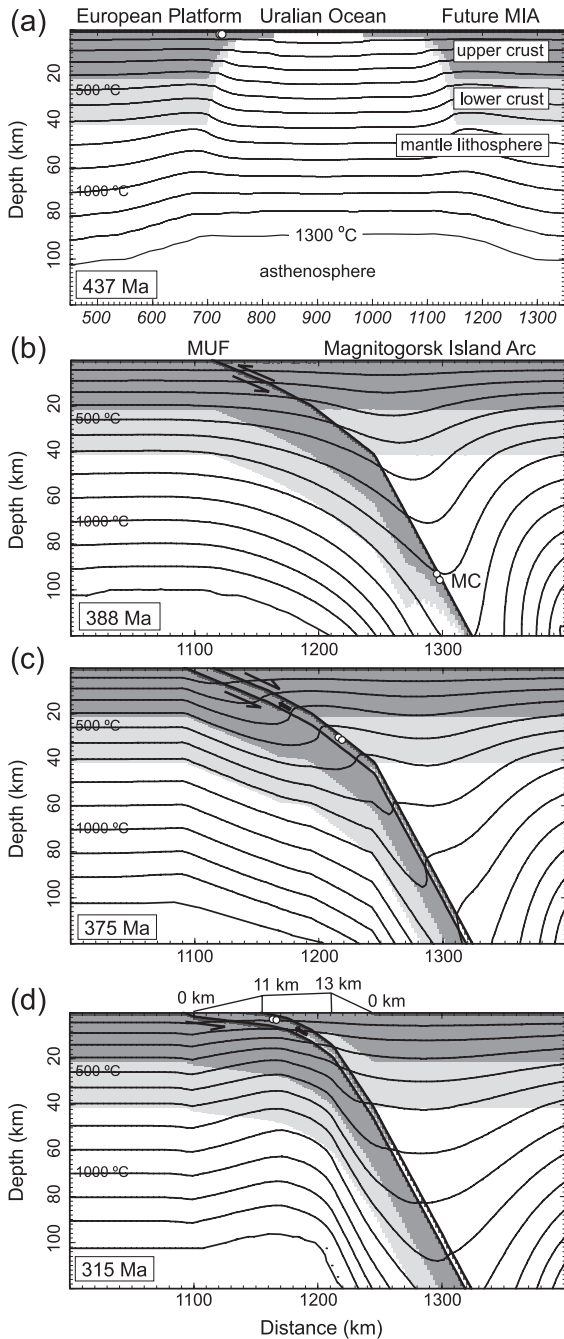
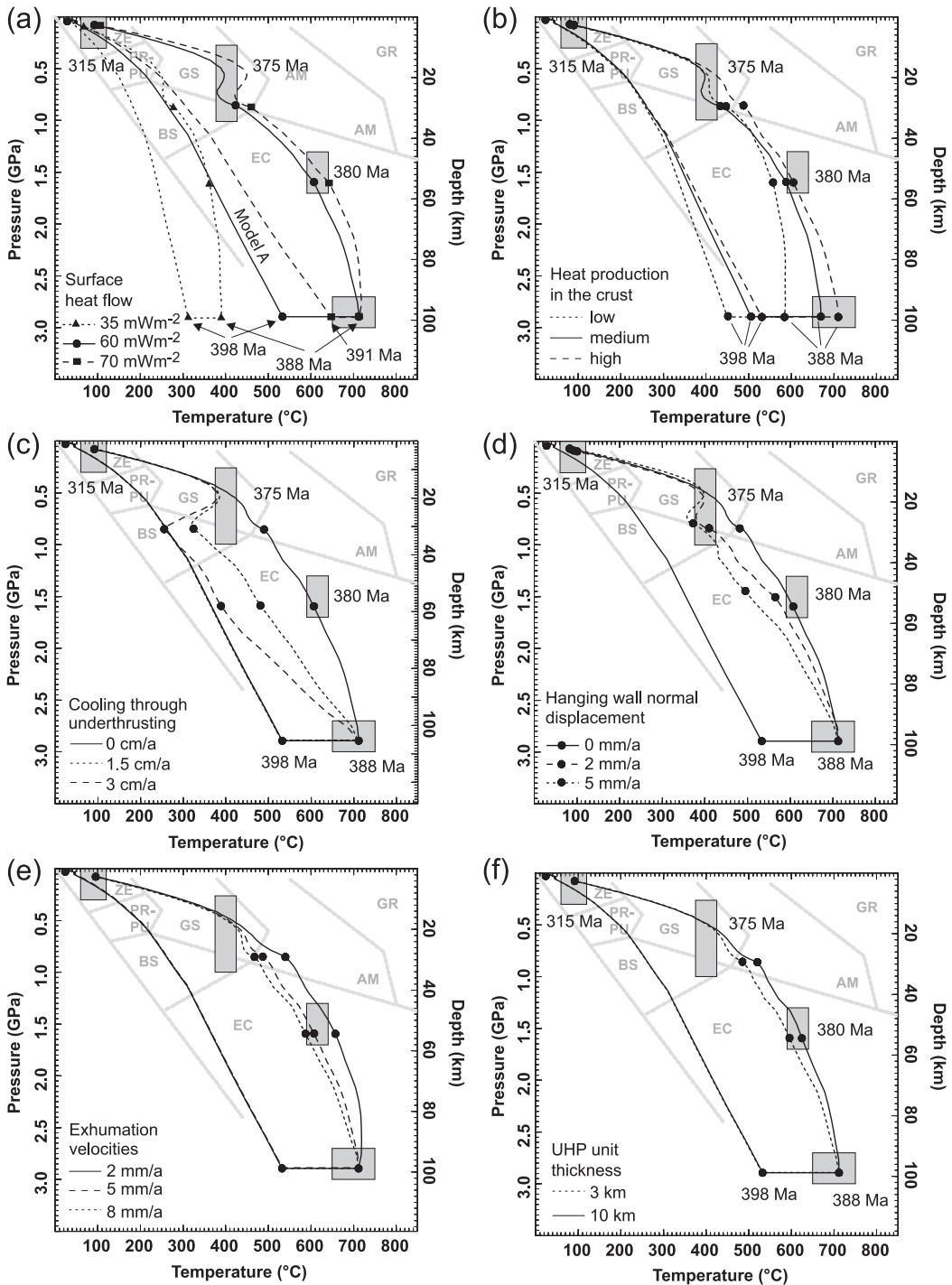


Fig. 3. Model A configurations for the Maksyutov UHP eclogite unit (MC). (a) Pre-subduction configuration immediately prior to the closure of the Uralian Ocean at 437 Ma. (b) UHP metamorphism at 388 Ma. (c) Syn-collisional exhumation to blueschist/greenschist-facies conditions at 375 Ma. (d) Cooling at 315 Ma, showing the amount of erosion during the last exhumation phase (375–315 Ma). White circles follow calculated  $P$ – $T$  path for the UHP unit; two points are shown to represent multiple locations within a rock volume which experience similar  $P$ – $T$  paths. Shading shows a sedimentary layer, upper crust, lower crust, and the subcrustal lithosphere, respectively, based on rheological stratification and model parameters listed in Table 2. Isotherms have a spacing of  $100$  °C. MUF, Main Uralian Fault; MIA, Magnitogorsk Island Arc.



recording cooling through 400–350 °C ( $T_c$  for Ar in phengite) and 420 °C ( $T_c$  for the U–Pb system in rutile). Because closure temperatures for Ar in white micas are well below peak metamorphic temperatures for Maksyutov, these ages represent cooling during exhumation. The majority of  $^{40}\text{Ar}/^{39}\text{Ar}$  data yield plateaus near 375 Ma [19]; because closure temperatures are better constrained in this system, we use 375 Ma in the modeling. We assume the UHP unit cooled to about 400 °C at 375 Ma during exhumation; this event is also recorded by a blueschist-/greenschist-facies metamorphic overprint in UHP unit rocks (see [3]).

Exhumation was syn-convergent and accomplished by a combination of west-directed thrusting and buoyant uplift of a small amount of dense eclogitic material within a largely buoyant quartzofeldspathic host rock (e.g., [23,24]). Apatite fission-track and  $^{40}\text{Ar}/^{39}\text{Ar}$  data indicate that the UHP unit cooled to 110 °C from 400 °C between 375 and 315 Ma [11].

The overall structure of the Maksyutov Complex is dominated by a NE–SW trending foliation and gentle folding about asymmetrical fold axes parallel to the dominant foliation; this large-scale fabric probably resulted from oblique convergence during the main collision in the south Urals [3]. Folding throughout the complex suggests that the main deformation phase occurred during exhumation after all units in Maksyutov were juxtaposed between about 335 and 315 Ma, after which all units were subjected to a common deformational and metamorphic history [3].

#### 4. Modeling methodology and model kinematics and limitations

Thermal conditions during Devonian and Carboniferous petrotectonic events in the south Urals may be determined using a kinematic, explicit three-step Runge–Kutta finite difference model that solves for the heat transfer equation in two dimensions. For a detailed description of the numerical model, see [25].

The model covers a rectangular area of 1800 km in length (Fig. 3a) by 250 km in depth with a regular grid spacing of 4.5 by 2.5 km. The lithosphere consists of an upper and lower crust with a thickness of 20 km each and a subcrustal lithosphere (Table 2, Fig. 3a). The lithosphere–asthenosphere boundary is defined by a temperature of 1300 °C, corresponding to the melting temperature of ultramafic rocks and is allowed to move according to imposed tectonic movements. Radiogenic heat production is assumed to be constant within each layer. The left and right hand sides of the numerical model are fixed ( $\delta T/\delta x=0$ ) during time integration. Material and thermal parameters used for the thermal modelling are listed in Table 2. Simple shear, pure shear, as well as combined shear tectonics are simulated based on a velocity field approach [25,28]. Simple shear kinematics are accounted for by moving blocks, separated by faults with different horizontal velocities, parallel to the fault plane. Faults are therefore pre-defined planes on the finite difference grid and separate velocity domains. The velocities are prescribed for individual time steps in agreement with the constraining data sets, and are constant within individual blocks. The amount of vertical motion is determined by the dip angle of the fault, which remains constant unless modified by surface processes like erosion or sedimentation. Vertical shear accommodates bending of layers where the dip changes.

The thermal evolution of the south Urals was modeled along an E–W transect (Fig. 1) based on early Paleozoic tectonic events [3,4]. The initial crustal thickness used was equal to the undeformed European Platform as imaged by deep seismic lines [29]. A thin layer of sediments (1.0 km thick) was added in the model to simulate passive margin sedimentation (see Fig. 3).

The Cambrian opening of the Uralian Ocean was accounted for in the modeling by pure shear extension (Table 1, Fig. 3a); after opening, the model was allowed to relax thermally until the onset of oceanic subduction during the Early Silurian as suggested by

Fig. 4. Thermal influence of (a) heat flow boundary conditions; (b) heat production in the crust; (c) cooling through underthrusting; (d) hanging wall normal displacement rates; (e) exhumation velocities; and (f) UHP unit thickness. (b)–(f) display results with initial heat flow boundary conditions of  $60 \text{ mW m}^{-2}$  as shown in (a). Except for (f), results have been calculated for a 5-km-thick UHP unit. Boxes show  $P$ – $T$  ranges for metamorphic events based on thermobarometry and isotopic data; ages shown correspond to the time at which the model reaches specific  $P$ – $T$  conditions. Metamorphic facies grid after [13]. Abbreviations: ZE=zeolite; PR-PU=prehnite–pumpellyite; GS=greenschist; BS=blueschist; AM=amphibolite; GR=granulite; EC=eclogite.

Table 2  
Thermal parameters used in the modeling

Layer	Rock analogue/ rheology	Thickness (km)	Density (kg m <sup>-3</sup> )	Conductivity (W m <sup>-1</sup> °C <sup>-1</sup> )	Specific heat (J kg <sup>-1</sup> °C <sup>-1</sup> )	Heat production (μW m <sup>-3</sup> )
Upper crust	Wet quartzite	20	2800	2.5	1050	0.800
Lower crust	Wet diorite	20	2900	2.5	1050	0.200
Mantle	Wet dunite	N.A.	3300	3.5	1050	0.002

Thermal parameters are taken from [26]; rock analogues are after [27]. Results for the heat production models are displayed in Fig. 3d.

the beginning of magmatic activity in the Magnitogorsk island arc [5,30]. Subduction of the Uralian Ocean was simulated by simple shear compression (Table 1, Fig. 3b).

The model subduction zone is represented by a pre-defined fault zone that accommodates horizontal shortening. Because melt generation occurs above the descending slab and the Maksyutov Complex is in the footwall of the subduction zone, we believe that formation of the Magnitogorsk island arc had no profound influence on the  $T-t$  evolution of the UHP unit; we therefore treat the Magnitogorsk island arc as a continental terrane. After subduction of the Uralian Ocean, the leading edge of the East European passive margin containing the UHP unit entered the subduction zone and was buried to 100 km which is the minimum depth for diamond formation in UHP metamorphic rocks (Fig. 3b). In the model, the timing of the UHP event was fixed at 388 Ma based on new U–Pb SHRIMP dating of zircons (see Fig. 2). After subduction to UHP depths, the model was allowed to thermally relax to reach the correct temperature conditions for metamorphism (Table 1). This relaxation period is interpreted to resemble detachment of the Maksyutov Complex from the downgoing plate and accretion to the upper plate. Mechanisms leading to the release of the accreted UHP unit allowing its return flow may be related to hydration of the mantle wedge [31].

After UHP metamorphism, exhumation of the UHP unit to HP eclogite-facies conditions at 380 Ma and subsequently to blueschist-/greenschist-facies conditions at about 375 Ma was simulated by reversing the motion along the fault plane (the model subduction zone) while propagating the subduction zone into footwall units (Fig. 3c). In this way, the UHP unit, which consists of a small amount of dense eclogitic material within largely quartzofeldspathic host rock, can be envisaged as a thrust sheet within the

subduction channel that is being exhumed buoyantly (e.g., [23,24]).

Final exhumation and cooling of the eclogites to the temperature range recorded by apatite fission track data (~110 °C at 315 Ma [11]) was modeled by a combination of erosion, accounting for half of the vertical motion, and west-directed thrusting (Fig. 3d). The amount of erosion is prescribed and proportional to the height of topography. Erosion rates are assumed to be constant during individual time steps.

In this study we used a kinematic numerical model to address key questions related to the thermal evolution of the Maksyutov Complex in the south Urals and its relationship to present-day heat flow data and UHP units in general. In this approach, the thermal effect of subduction or exhumation processes is studied in a kinematic framework allowing for a high degree of freedom in testing a variety of potentially important parameters for the thermal evolution of UHP complexes. As such we do not aim to answer questions concerning the dynamics of subduction and UHP exhumation like exploring the driving forces for the exhumation of UHP complexes. Recent numerical, analytical, and physical modeling studies suggest that exhumation of UHP rocks to crustal levels is primarily driven by buoyancy forces or forced flow within the subduction channel, whereas processes such as erosion or detachment faulting are more important for the final exhumation phase [23,31–34]. We therefore adopt thrusting and erosion as simplified exhumation mechanisms in our models.

Because of significant uncertainties in shear parameters, i.e., shear stresses in subduction zone environments are estimated to range between 0 and 100 MPa (see [35] for a discussion), we did not include shear heating in the model. Numerical modeling studies on the thermal structure of subduction zones and UHP metamorphism indicate that depending on the amount of shear stress and subduction velocity, shear heating



might increase the temperature at the subduction shear zone by up to 200 °C [26,36]. Microstructural arguments, however, like the predominance of deformation mechanisms including dissolution precipitation creep and fluid assisted granular flow during high-pressure deformation suggest that the flow strength of rocks in parts of the subduction channel might be very low [37,38], thereby limiting the thermal contribution of shear heating. Other difficult to constrain parameters like the thermal effects of metamorphic reactions and fluid circulation with the subduction channel are ignored in this study.

## 5. Modeling results

Modeling results are described with respect to our reference model A, which was successful in reproduc-

ing the  $P$ – $T$ – $t$  path of the Maksyutov Complex; relevant thermal parameters are listed in Tables 2 and 3. Fig. 4 shows the predicted  $P$ – $T$ – $t$  paths for model A (the “best-fit” model; Fig. 4a) and for models exploring the thermal influence of various model parameters listed in Table 3.

### 5.1. Heat flow and heat production (Fig. 4a,b; Table 3)

In the Ural Mountains and adjacent European Platform, surface heat flow is low with an average of 35 mW m<sup>-2</sup> and is mainly attributed to the low radiogenic heat production in the crust [2]. For the modeling, we increased the average of modern heat production data [2] by a factor of 1.2 to account for higher heat production in the Devonian [39]. Heat flow values in Table 3 represent initial conditions where heat flow is distributed uniformly across the

Table 3  
Overview of parameters changed in the modelling

Surface heat flow (mW m <sup>-2</sup> )	Heat flux from asthenosphere (mW m <sup>-2</sup> )	Heat production in the upper crust (μW m <sup>-3</sup> )	Rate of underthrusting (cm/year) 380–380/380–375 Ma	Hanging wall normal displacement (cm/year) 388–375 Ma	Exhumation rate (cm/year) 388–380/380–375 Ma	UHP unit thickness (km)
<i>Heat flow models</i>						
60	40	0.8	0/1.5	0	0.5/0.45	5
70	50	0.8	0/1.5	0	0.5/0.45	5
35	15	0.8	0/1.5	0	0.5/0.45	5
<i>Radiogenic heat production in the upper crust</i>						
60	40	Low—0.8	0/1.5	0	0.5/0.45	5
60	36	Medium—1.0	0/1.5	0	0.5/0.45	5
60	26	High—1.5	0/1.5	0	0.5/0.45	5
<i>Cooling through underthrusting</i>						
60	40	0.8	0/0	0	0.5/0.45	5
60	40	0.8	1.5/1.5	0	0.5/0.45	5
60	40	0.8	3/3	0	0.5/0.45	5
<i>Cooling through normal faulting in the hanging wall</i>						
60	40	0.8	0/0	0	0.5/0.45	5
60	40	0.8	0/0	0.2	0.5/0.45	5
60	40	0.8	0/0	0.5	0.5/0.45	5
<i>Influence of exhumation velocity</i>						
60	40	0.8	0/0	0	0.2/0.2	5
60	40	0.8	0/0	0	0.45/0.45	5
60	40	0.8	0/0	0	0.8/0.8	5
<i>Influence of UHP unit thickness</i>						
60	40	0.8	0/0	0	0.5/0.45	3
60	40	0.8	0/0	0	0.5/0.45	10

model; these values are subject to lateral variations across the orogen during time integration.

The best fit  $P$ – $T$ – $t$  path is achieved using an initial surface heat flow value of  $60 \text{ mW m}^{-2}$  (Model A, Fig. 4a) and heat flow of  $40 \text{ mW m}^{-2}$  at the lithosphere–asthenosphere boundary (Table 3). For these thermal boundary conditions the  $P$ – $T$ – $t$  history of the UHP unit is reproducible within the constraining petrological and radiometric data sets (see Section 3). The  $P$ – $T$ – $t$  path of Model A is characterized by moderate heating during subduction, isobaric heating during a 10 my relaxation phase, continuous cooling during the exhumation of the UHP unit from mantle (~100 km) to lower crustal (~30 km) depths, and isothermal exhumation followed by slow cooling during final exhumation to shallow crustal levels (~4 km). Sensitivity tests suggest that the age of a subducting ocean and the subduction velocity only effect the temperature of the UHP unit at the end of the burial phase (see [35]) and have little thermal effect on the succeeding exhumation phase. Subsequent thermal relaxation is required to attain the proper temperature conditions for UHP metamorphism (Figs. 3b and 4a). Other models using present-day heat flow values ( $35 \text{ mW m}^{-2}$ ; Fig. 4a) never yielded the observed  $P$ – $T$  conditions; even full thermal relaxation (>100 my) resulted in model temperatures that were too low for eclogite-facies metamorphism. Higher initial heat flow boundary conditions ( $70 \text{ mW m}^{-2}$ ; Fig. 4a) lead to UHP metamorphic conditions soon after (2 my) the end of the burial phase but do not accurately track the retrograde  $P$ – $T$  path (Fig. 4a).

Radiogenic heat production within the upper crust of the south Ural transect (see Fig. 1) is low, with a mean value of  $0.66 \mu\text{W m}^{-3}$  [2], due to the predominance of mafic rocks in the Magnitogorsk zone. This value is representative of the modern structure of the Urals (Fig. 1) but does not necessarily reflect ancient heat production within the UHP unit, a passive continental margin segment of East European origin. Model simulations with different heat production values (Table 3) were performed to assess the influence of higher heat production in the upper crust on the thermal history of the UHP unit.

In the numerical model, steady state heat flow at the surface is balanced by the amount of heat flux from the asthenosphere and the amount of heat

production within the different model layers (see Fig. 3). Increasing the heat production in the upper crust therefore requires less heat flux from the asthenosphere to maintain the same heat flow at the surface. Consequently, models with high heat production in the upper crust (and hence less influx from the asthenosphere) yield too low temperatures at the end of the subduction phase (Fig. 4b); this suggests that the lower heat flux from the mantle overcompensates for the heat gain due to higher radioactive heat production resulting in a net temperature loss of about  $80 \text{ }^\circ\text{C}$  with respect to model A. The opposite is true for the exhumation phase where the influence of the low heat flux from the asthenosphere decreases relative to the heat production within the crust as indicated by the converging  $P$ – $T$  paths during decompression (Fig. 4b).

### 5.2. Cooling of the UHP unit during decompression (Fig. 4c)

$P$ – $T$  data from the Maksyutov Complex document continuous cooling during exhumation from UHP to near-surface positions. In the following paragraphs, we present sensitivity tests that aim to evaluate the importance of contemporaneously active processes such as underthrusting or normal faulting in the hanging wall of the MUF as well as variations of parameters including UHP unit thickness and exhumation velocity on the temperature evolution of the UHP unit during decompression.

### 5.3. Cooling through underthrusting and normal faulting in the hanging wall (Fig. 4c,d; Table 3)

The UHP unit cooled by about  $300 \text{ }^\circ\text{C}$  between 388 and 375 Ma. Modeling results suggest that continued subduction in the footwall is an efficient mechanism to cool the UHP unit with the rate of subduction being the controlling factor (Fig. 4c). The calculated  $P$ – $T$ – $t$  paths also show that for the Maksyutov Complex, no additional cooling is required during exhumation of the UHP unit from UHP to HP conditions. During this phase, conductive cooling is more efficient than heat advection induced by the upward movement of the UHP unit and hence results in temperature decrease of about  $100 \text{ }^\circ\text{C}$  to 380 Ma. However, subsequent exhumation to blues-

chist-/greenschist-facies metamorphic conditions at 375 Ma, requires additional mechanisms to reproduce the  $P$ – $T$  path constrained by the data. Relatively slow underthrusting at rates of 1.5 cm/year (Model A in Fig. 4a) provides enough cooling to predict blueschist-/greenschist-facies conditions. Similar rate-dependent relationships are observed if we cool through normal faulting in the hanging wall of the UHP unit (Fig. 4d). In this case, which simulates normal fault activity along the MUF, downward motion of the hanging wall block induces cooling by means of underthrusting.

#### 5.4. Exhumation velocity and UHP unit thickness (Fig. 4e,f; Table 3)

As outlined in the previous sections, exhumation proceeds in three stages in Model A (Fig. 4): (1) from UHP conditions at 388 Ma to HP eclogite-facies conditions at 380 Ma; (2) from HP eclogite-facies conditions to blueschist-/greenschist-facies conditions at 375 Ma; and (3) from blueschist-/greenschist-facies conditions to the uppermost crust at 315 Ma. Exhumation rates for the first two stages of exhumation are quite modest at 5 and 4.5 mm/year, respectively (Fig. 4a). The exhumation rate for the UHP unit after the blueschist-/greenschist-facies overprint was much slower (~0.47 mm/year, Table 1) allowing the thermal structure to largely re-equilibrate in the upper crust, while the deep thermal structure was still controlled by underthrusting (Fig. 3d). Slowing exhumation by a factor of 10 and applying erosion yields nearly isothermal exhumation of the UHP unit for a period of ~20 my (Model A, Fig. 4a). Thereafter, cooling accelerates due to the proximity of the earth's surface. According to the model predictions, the eclogites were at a depth of 3–4 km when they cooled to below 110 °C suggesting that 3–4 km of material has eroded since the Late Carboniferous (315 Ma).

Higher exhumation rates from UHP to blueschist-/greenschist-facies conditions shift the predicted  $P$ – $T$  path slightly toward lower temperatures, whereas slower exhumation rates increase temperatures due to the decreasing influence of heat advection (Fig. 4e). In our modelling, the  $P$ – $T$  paths followed are near the boundary with the upper plate where thermal gradients across the UHP unit are very high. Particularly in the case of fast exhumation (8 mm/year), con-

ductive heat loss to the upper (cooler) plate is enhanced, yielding slightly cooler exhumation paths. The efficiency of conductive cooling during exhumation is, therefore, also a function of the position of the rock within the UHP unit.

Model runs with different UHP unit thicknesses (3, 5, and 10 km), appropriate for the south Urals, suggest that this parameter is less important for the decompression-related thermal history of the UHP unit than, for example, contemporaneous underthrusting (compare Fig. 4a and f with c). As thicker UHP units have a higher capacity to advect heat and conductive cooling takes longer to effect the entire unit, models with thicker UHP units yield warmer exhumation paths. Our modeling results are consistent with those of [36] although distinct temperature differences at the onset of exhumation in their models exploring the same parameter seems to overstate its importance. Modeling shown in Fig. 4f indicates that UHP unit thickness of 3–10 km are reasonable; we use 5 km for Model A as an intermediate value that meets all  $P$ – $T$ – $t$  criteria.

## 6. Discussion of modeling results

### 6.1. Paleo- vs. modern heat flow

The  $P$ – $T$ – $t$  evolution of the Maksyutov UHP unit cannot be explained unless heat flow has varied over time. Our modeling shows that syn-orogenic heat flow (400–315 Ma) must have been much higher than present-day heat flow; an initial surface heat flow value of 60 mW m<sup>-2</sup> closely reproduces the  $P$ – $T$  path of the UHP unit. In other regions such as the European Alps where UHP metamorphism of the Dora Maira massif occurred during Tertiary collision (e.g., [40]), modern surface heat flow data range between 50 and 80 mW m<sup>-2</sup> [41]. Our modeling predictions are consistent with these data and underline the relevance of the chosen heat flow boundary conditions for the thermal evolution of the Maksyutov Complex. Since the Carboniferous, decay of the transient thermal perturbation related to orogenic activity, together with the decreasing radiogenic productivity and paleo-climate influences (see [2]), led to the very low modern heat flow values.

### 6.2. Shear heating

Thermal modeling studies of subduction zone environments suggest that transient heat sources such as shear heating can increase subduction zone temperatures by up to 200 °C depending on the prevailing shear stresses and the imposed velocity along subduction- and/or exhumation-related shear zones [35,36]. In the Maksyutov Complex, shear heating may have permitted UHP metamorphism under lower heat flow conditions than suggested by our modeling. Subsequent exhumation of the UHP unit must then have been accompanied by a combination of cooling processes to obtain the  $P$ – $T$  path recorded by the rocks. However, the Maksyutov UHP unit consists of small eclogite lenses within dominantly quartzofeldspathic rocks. The quartzofeldspathic matrix deforms around eclogite lenses protecting eclogite from significant shearing; the cores of eclogite bodies appear largely undeformed [3]. Shear stresses estimated for similar eclogite/country rock relationships observed in the Dora Maira Massif are estimated to be only 2 MPa, at 700 °C and strain rates of  $10^{-15} \text{ s}^{-1}$  Stöckhert and Renner [37]. Such low shear stresses are considered insufficient to cause a considerable temperature increase due to shear heating [35]. Furthermore, exhumation rates for most UHP complexes are on the order of 1–2 cm/year ([42] and references therein). We estimate the maximum exhumation rate for the Maksyutov Complex is 5 mm/year, and is therefore a “low velocity” end member among UHP complexes. The shear zone velocity applicable to the Maksyutov Complex is probably too low to cause significant shear heating.

### 6.3. Cooling during exhumation

Different mechanisms have been proposed for rapid cooling during the exhumation of UHP terranes, a prerequisite for the preservation of UHP index minerals like coesite and diamond [43]. Among those mechanisms we consider, based on our modeling study, cooling through underthrusting of the subducting slab as most efficient (Fig. 4c). Additionally, a cool exhumation environment is favored in case of concomitant normal displacement of hanging wall units and low radiogenic heat

production in the crust, whereas for our set of boundary conditions other parameters like unit thickness or exhumation rate turned out to be less important. Our findings are consistent with numerical modeling studies of Peacock [44] or Roselle and Engi [36], although the latter regard “unit thickness” as a controlling parameter.

Exhumation of Maksyutov UHP rocks proceeded in multiple stages. We infer from the modeling that conditions favoring cooling of the UHP Maksyutov Complex during exhumation include low crustal heat production (Fig. 4b; [2,45]), a relatively thin tectonic unit (3–10 km), moderate exhumation rates (~5.0 mm/year; Fig. 4e), and a small amount of cooling through underthrusting of the subducting slab (Fig. 4c). In the absence of heat-producing mechanisms such as shear heating only a limited amount of additional cooling is required during exhumation from HP to greenschist-/blueschist-facies conditions to fit the  $P$ – $T$  path; this cooling could either stem from underthrusting of cold footwall, normal displacement of hanging wall units, or a combination of both (compare Model A in Fig. 4a with Fig. 4d). Our thermal calculations furthermore suggest that the blueschist-/greenschist-facies metamorphic overprint at ~375 Ma occurred in the lower crust (~32–28 km) and not the mid-crust (~20 km) as suggested by Hetzel and Romer [45]. According to our modeling results, cooling of the UHP unit might have been interrupted by approximately isothermal exhumation during the first 20 my of the last exhumation phase (375–315 Ma). During this time period, when exhumation velocities had decreased considerably (Table 1), re-equilibration of the thermal structure due to heat conduction dominates over exhumation-related advective heat transport. Final exhumation to shallow crustal levels was accompanied by cooling and further thermal re-equilibration in the upper crust. The UHP unit reached shallow crustal levels (3–4 km) during the early Late Carboniferous, thus constraining the denudation rate until present.

The exhumation rate of ca. 5.0 mm/year as inferred for the Maksyutov Complex is much slower than estimates for many other UHP complexes; for example, exhumation rates for the Dabie Shan (eastern China) are estimated to be up to 25 mm/year [46] and those of the Dora Maira Massif

(European Alps) range from 20–24 mm/year [40]; this clearly shows that the rare preservation of UHP index minerals in the Maksyutov Complex is not primarily controlled by the exhumation velocity. Very slow exhumation on the other hand (0.3–1.5 mm/year as suggested by Leech and Stockli [11], to pseudomorphose diamonds) hampers cooling, yields too high temperatures in our models, and fails to achieve the HP eclogite  $P$ – $T$  conditions (Fig. 4e). It follows that in the absence of efficient cooling mechanisms, early phases of decompression will be accompanied by heating, not cooling, in cases when the subduction related thermal perturbation restores faster than the rocks exhume. Although different exhumation rates yield slightly deviating cooling paths, we concur with [36,44] who consider exhumation velocities a parameter of secondary importance for the thermal evolution of exhuming UHP units.

## 7. Conclusions

New U–Pb SHRIMP data from zircon dates UHP metamorphism of the Maksyutov Complex at  $388 \pm 4$  Ma. This early date changes the  $P$ – $T$ – $t$  history for Maksyutov; our thermal modeling tests assumptions about the evolution of this UHP subduction zone complex, and by inference, all UHP complexes. Thermal modeling of the Maksyutov Complex shows that modern heat flow data cannot be used as a valid assumption for reconstructing and discussing the  $P$ – $T$ – $t$  history of UHP metamorphic rocks in the context of Paleozoic subduction and collision in the Urals. Conversely, quantification of the thermal evolution of UHP units, most of which are of Paleozoic age (e.g., [47]), needs to account for the strong time dependence of the lithospheric thermal structure.

The preservation of UHP index minerals demands cooling during decompression; our modeling suggests that cooling during exhumation is favored when concomitant subduction/underthrusting or normal faulting in the hanging wall takes place, the UHP unit is thin, and radiogenic heat production is low. In contrast to a widespread perception, fast exhumation is not required for the preservation of UHP minerals as shown by the example of the

Maksyutov Complex in the south Urals, which was exhumed to mid-crustal levels at a comparably slow rate (~5 mm/year).

## Acknowledgments

Funding for this work was provided by the National Science Foundation grant INT-99001573 to Leech and by NWO-ALW project no. 810.31.003 (Willingshofer). We are grateful to Ellen Metzger and Ruth Zhang for help with SHRIMP analyses and to J.D. van Wees for providing the numerical code. Many thanks to Onno Oncken, Susan Ellis, Sierd Cloetingh, Simon Klemperer, and two anonymous reviewer for helpful comments.

## References

- [1] W.G. Ernst, S. Maruyama, S. Wallis, Buoyancy-driven, rapid exhumation of ultrahigh-pressure metamorphosed continental crust, *Proc. Natl. Acad. Sci.* 94 (1997) 9532–9537.
- [2] I.T. Kukkonen, I.V. Golovanova, Y.V. Khachay, V.S. Drushinin, A.M. Kosarev, V.A. Schapov, Low geothermal heat flow of the Urals fold belt: Implication of low heat production, fluid circulation or palaeoclimate? *Tectonophysics* 162 (1997) 63–85.
- [3] M.L. Leech, W.G. Ernst, Petrotectonic evolution of the high-to ultrahigh-pressure Maksyutov Complex, Karayanova area, south Ural Mountains: structural and oxygen isotope constraints, *Lithos* 52 (2000) 235–252.
- [4] D. Brown, C. Juhlin, J. Alvarez-Marron, A. Pérez-Estaún, A. Oslianski, Crustal-scale structure and evolution of an arc-continent collision zone in the southern Urals Russia, *Tectonics* 17 (1998) 158–171.
- [5] G.N. Savelieva, R.W. Nesbitt, A synthesis of the stratigraphic and tectonic setting of the Uralian ophiolites, *J. Geol. Soc. (Lond.)* 153 (1996) 525–537.
- [6] A.V. Maslov, B.D. Erdtmann, K.S. Ivanov, S.N. Ivanov, M.T. Krupenin, The main tectonic events, depositional history, and the palaeogeography of the Southern Urals during the Riphean-early Palaeozoic, *Tectonophysics* 276 (1997) 313–335.
- [7] V.N. Puchkov, Structure and geodynamics of the Uralian orogen, in: J.-P. Burg, M. Ford (Eds.), *Orogeny Through Time*, Geological Society Special Publication, vol. 121, 1997, pp. 201–236.
- [8] M.L. Leech, E.P. Metzger, J.L. Wooden, R.E. Jones, C.L. Schwartz, R.J. Beane, New eclogitization and protolith ages for the Maksyutov Complex (south Ural Mountains) based on U–Pb zircon SHRIMP data, *Eos Trans., Am. Geophys. Union* 83 (2002).

- [9] R.L. Edwards, G.J. Wasserburg, The age and emplacement of obducted oceanic crust in the Urals from Sm–Nd and Rb–Sr systematics, *Earth Planet. Sci. Lett.* 72 (1985) 389–404.
- [10] L.P. Zonenshain, V.G. Korinevsky, V.G. Kazmin, D.M. Pechersky, V.V. Khain, V.V. Matveenkov, Plate tectonic model of the south Urals development, *Tectonophysics* 109 (1984) 95–135.
- [11] M.L. Leech, D.F. Stockli, The late exhumation history of the ultrahigh pressure Maksyutov Complex, south Ural Mountains, from new apatite fission-track data, *Tectonics* 19 (2000) 153–167.
- [12] H.P. Echter, R. Hetzel, Main Uralian thrust and main Uralian normal fault: non-extensional palaeozoic high-P rock exhumation, oblique collision, and normal faulting in the southern Urals, *Terra Nova* 9 (1997) 158–162.
- [13] F.S. Spear, Metamorphic phase equilibria and pressure–temperature–time paths, *Monogr.-Mineral. Soc. Am.* (1994) 799.
- [14] B.V. Chesnokov, V.A. Popov, Increasing volume of quartz grains in eclogites of the South Urals, *Dokl. Akad. Nauk SSSR* 162 (1965) 176–178.
- [15] N.L. Dobretsov, L.V. Dobretsova, New mineralogic data on the Maksyutov eclogite–glaucophane schist complex, southern Urals, *Dokl. Akad. Nauk SSSR* 300 (1988) 111–116.
- [16] M.L. Leech, W.G. Ernst, Graphite pseudomorphs after diamond? A carbon isotope and spectroscopic study of graphite cuboids from the Maksyutov complex, south Ural Mountains, Russia, *Geochim. Cosmochim. Acta* 62 (1998) 2143–2154.
- [17] B. Bostick, R.E. Jones, W.G. Ernst, C. Chen, M.L. Leech, R.J. Beane, Low-temperature microdiamond aggregates in the Maksyutov metamorphic complex, south Ural Mountains, Russia, *Am. Mineral.* 88 (2003) 1709–1717.
- [18] V.S. Shatsky, E. Jagoutz, O.A. Koz'menko, Sm–Nd dating of the high-pressure metamorphism of the Maksyutov Complex, southern Urals, *Trans. Russ. Acad. Sci.* 353 (1997) 285–288.
- [19] R.J. Beane, J.N. Connelly,  $^{40}\text{Ar}/^{39}\text{Ar}$ , U–Pb, and Sm–Nd constraints on the timing of metamorphic events in the Maksyutov complex southern Ural mountains, *J. Geol. Soc. (Lond.)* 157 (2000) 811–822.
- [20] J. Glodny, B. Bingen, H. Austrheim, J.F. Molina, A. Rusin, Precise eclogitization ages deduced from Rb/Sr mineral systematics: The Maksyutov complex, Southern Urals, Russia, *Geochim. Cosmochim. Acta* 66 (2002) 1221–1235.
- [21] J. Glodny, H. Austrheim, J.F. Molina, A. Rusin, D. Seward, Rb/Sr record or fluid–rock interaction in eclogites: The Marun–Keu complex, polar Urals, Russia, *Geochim. Cosmochim. Acta*, in press.
- [22] P. Matte, H. Maluski, R. Caby, A. Nicholas, P. Kepezhinkskas, S. Sobolev, Geodynamic model and  $^{39}\text{Ar}/^{40}\text{Ar}$  dating for the generation and emplacement of the high pressure metamorphic rocks in SW Urals, *C. R. Acad. Sci., Paris* 317 (1993) 1667–1674.
- [23] A. Chemenda, P. Matte, V. Sokolov, A model of Palaeozoic obduction and exhumation of high-pressure/low-temperature rocks in the southern Urals, *Tectonophysics* 276 (1997) 217–227.
- [24] M.L. Leech, Arrested orogenic development: eclogitization, delamination, and tectonic collapse, *Earth Planet. Sci. Lett.* 185 (2001) 149–159.
- [25] J.D. van Wees, K. de Jong, S. Cloetingh, Two-dimensional  $P$ – $T$ – $t$  modelling and the dynamics of extension and inversion in the Betic Zone (SE Spain), *Tectonophysics* 203 (1992) 305–324.
- [26] H.N. Pollack, D.S. Chapman, On the regional variation of heat flow, geotherms and lithospheric thickness, *Tectonophysics* 38 (1977) 279–296.
- [27] N. Carter, M. Tsenn, Flow properties of continental lithosphere, *Tectonophysics* 136 (1987) 27–63.
- [28] W.R. Buck, F. Martinez, M.S. Steckler, J.R. Cochran, Thermal consequences of lithospheric extension; pure and simple, *Tectonics* 7 (1988) 213–234.
- [29] R. Berzin, O. Oncken, J.H. Knapp, A. Perez-Estaun, T. Hismatulin, N. Yunosov, A. Lipilin, Orogenic evolution of the Ural mountains: results from an integrated seismic experiment, *Science* 274 (1996) 220–221.
- [30] L.P. Zonenshain, M.I. Kuzmin, L.M. Natapov, *Geology of the USSR: a plate tectonic synthesis*, American Geophysical Union Geodynamics Series, Washington, DC, 1990, 242 pp.
- [31] T. Gerya, B. Stöckhert, A.L. Perchuk, Exhumation of high-pressure metamorphic rocks in a subduction channel: a numerical simulation, *Tectonics* 21 (2002) 1056.
- [32] E. Burov, L. Jolivet, L. Le Pourhiet, A. Poliakov, A thermo-mechanical model of exhumation of high pressure (HP) and ultra-high pressure (UHP) metamorphic rocks in Alpine-type collision belts, *Tectonophysics* 342 (2001) 113–136.
- [33] M.-P. Doin, P. Henry, Subduction initiation and continental crust recycling: the roles of rheology and eclogitization, *Tectonophysics* 342 (2001) 163–191.
- [34] T. Gerya, B. Stöckhert, Exhumation rates of high pressure metamorphic rocks in subduction channels: the effect of rheology, *Geophys. Res. Lett.* 29 (2002) 1261.
- [35] S.M. Peacock, Thermal and petrologic structure of subduction zones, in: G.E. Bebout, D.W. Scholl, S.H. Kirby, J.P. Platt (Eds.), *Subduction Top to Bottom*, Am. Geophys. Union Geophys. Monogr., vol. 96, 1996, pp. 119–133.
- [36] G.T. Roselle, M. Engi, Ultra high pressure (UHP) terrains: lessons from thermal modeling, *Am. J. Sci.* 302 (2002) 410–441.
- [37] B. Stöckhert, J. Renner, Rheology of crustal rocks at ultrahigh pressure, in: B.R. Hacker, J.G. Liou (Eds.), *When Continents Collide: Geodynamics and Geochemistry of Ultrahigh-Pressure Rocks*, Kluwer, New York, 1998, pp. 67–95.
- [38] B. Stöckhert, Stress and deformation in subduction zones: insight from the record of exhumed metamorphic rocks, in: S. de Meer, M.R. Drury, J.H.P. de Bresser, G.M. Pennock (Eds.), *Deformation Mechanisms, Rheology and Tectonics: current status and future perspectives*, Spec. Publ.-Geol. Soc. Lond., vol. 200, 2002, pp. 255–274.
- [39] W.R. van Schmus, Natural radioactivity of the crust and mantle, *Global Earth Physics: A Handbook of Physical Constants*, American Geophysical Union, 1995, pp. 283–291.
- [40] D. Gebauer, H.-P. Schertl, M. Brix, W. Schreyer, 35 Ma old ultrahigh-pressure metamorphism and evidence for rapid

- exhumation in the Dora maira Massif, western Alps, *Lithos* 41 (1997) 5–24.
- [41] E. Hurtig, V. Cermak, R. Haenel, V.I. Zvi, *Geothermal Atlas of Europe*, Herman Haak Verlag, Potsdam, Germany, 1991.
- [42] C. Chopin, Ultrahigh-pressure metamorphism: tracing continental crust into the mantle, *Earth Planet. Sci. Lett.* 212 (2003) 1–14.
- [43] W.G. Ernst, S.M. Peacock, A thermotectonic model for preservation of ultrahigh-pressure phases in metamorphosed continental crust, in: G.E. Bebout, D.W. Scholl, S.H. Kirby, J.P. Platt (Eds.), *Subduction Top to Bottom*, *Am. Geophys. Union Geophys. Monogr.*, vol. 96, 1996, pp. 171–178.
- [44] S.M. Peacock, Ultrahigh-pressure metamorphic rocks and the thermal evolution of continent collision belts, *Isl. Arc* 4 (1995) 376–383.
- [45] R. Hetzel, R.L. Romer, A moderate exhumation rate for the high-pressure Maksyutov Complex, southern Urals, Russia, *Geol. J.* 35 (2000) 327–344.
- [46] L.E. Webb, B.R. Hacker, L. Ratschbacher, M.O. McWilliams, S.W. Dong, Thermochronologic constraints on deformation and cooling history of high- and ultrahigh-pressure rocks in the Qinling–Dabie orogen, eastern China, *Tectonics* 18 (1999) 621–638.
- [47] D. Rumble, J.G. Liou, B.M. Jahn, Continental crust subduction and ultrahigh pressure metamorphism, in: R. Rudnick (Ed.), *Treatise on Geochemistry*, vol. 3 *The Crust*, Elsevier, Amsterdam, 2003, pp. 293–319.